REPORT

# The Rubble-Pile Asteroid Itokawa as Observed by Hayabusa

A. Fujiwara,[1]* J. Kawaguchi,[1] D. K. Yeomans,[2] M. Abe,[1] T. Mukai,[3] T. Okada,[1] J. Saito,[1] H. Yano,[1] M. Yoshikawa,[1] D. J. Scheeres,[4] O. Barnouin-Jha,[5] A. F. Cheng,[5] H. Demura,[6] R. W. Gaskell,[2] N. Hirata,[3] H. Ikeda,[1] T. Kominato,[7] H. Miyamoto,[8] A. M. Nakamura,[3] R. Nakamura,[9] S. Sasaki,[10] K. Uesugi[1]

During the interval from September through early December 2005, the Hayabusa spacecraft was in close proximity to near-Earth asteroid 25143 Itokawa, and a variety of data were taken on its shape, mass, and surface topography as well as its mineralogic and elemental abundances. The asteroid's orthogonal axes are 535, 294, and 209 meters, the mass is $3.51 \times 10^{10}$ kilograms, and the estimated bulk density is $1.9 \pm 0.13$ grams per cubic centimeter. The correspondence between the smooth areas on the surface (Muses Sea and Sagamihara) and the gravitationally low regions suggests mass movement and an effective resurfacing process by impact jolting. Itokawa is considered to be a rubble-pile body because of its low bulk density, high porosity, boulder-rich appearance, and shape. The existence of very large boulders and pillars suggests an early collisional breakup of a preexisting parent asteroid followed by a re-agglomeration into a rubble-pile object.

The Hayabusa (the original code name was MUSES-C) engineering spacecraft, launched by the fifth Mu V launch vehicle on 9 May 2003 [hereafter universal time coordinated (UTC) times are noted], was designed to acquire samples from the surface of near-Earth asteroid 25143 Itokawa (1998 SF36) and return them to Earth. The main objectives of the mission were to demonstrate the performance of various technical items such as ion engines, autonomous navigation, sampling of the asteroid's surface, and high-speed reentry into the Earth's atmosphere (*1*). In addition, important scientific results were expected from this mission.

Primitive asteroids are key objects in the research of the early planetary system evolution process. Spectroscopic observations of asteroids have resulted in about a dozen spectral classes. To draw a first-order big picture for the whole asteroid region, we need to know the physical properties of asteroids of each spectral class and to assign each class to a corresponding meteorite group. This is possible by sending a small number of spacecraft to well-selected asteroids that are individual representatives of the major spectral types. Once this is achieved, we can make maximum use of the abundant meteorite data to understand the origin and the evolution of the corresponding spectral class of asteroids. This sample return mission was intended to initiate this program.

Before the final selection of Itokawa, the target asteroid was changed twice because of changes in mission scenarios and a delay in the spacecraft launch schedule. Itokawa, an Apollo asteroid discovered in 1998, follows its orbital path from 0.9530 astronomical units (AU) just inside the Earth's orbit to 1.6947 AU just outside of the orbit of Mars. Its orbit allows close encounters with the Earth, a circumstance that provides frequent opportunities for ground-based observations. Photometric observations (*2*, *3*) and radar observation (*4*) provided the initial shape models; the rotational period was found to be 12.1 hours, the rotation axis is almost perpendicular to the ecliptic plane, and the rotation direction is retrograde. Spectrally, Itokawa is classified as an S-type asteroid, a type common in the inner portion of the asteroid belt. The surface mineralogy is apparently dominated by silicates (pyroxene and olivine) and Fe metal (*5*). Hence, spectral observations of Itokawa were expected to form baseline measurements representative of these common asteroids. However, this asteroid was selected primarily because it is one of the most accessible targets for the low-energy launch vehicle.

One crucial issue in the current asteroid research is the puzzle of the rubble-pile structure. Although some asteroid researchers have supposed that most of the asteroids larger than about 1 km in size should be rubble piles, there has been no definite evidence of the rubble-pile structure for any of the asteroids observed to date by spacecraft.

Hayabusa's trajectory to the asteroid is illustrated in Fig. 1A. After cruising with nearly

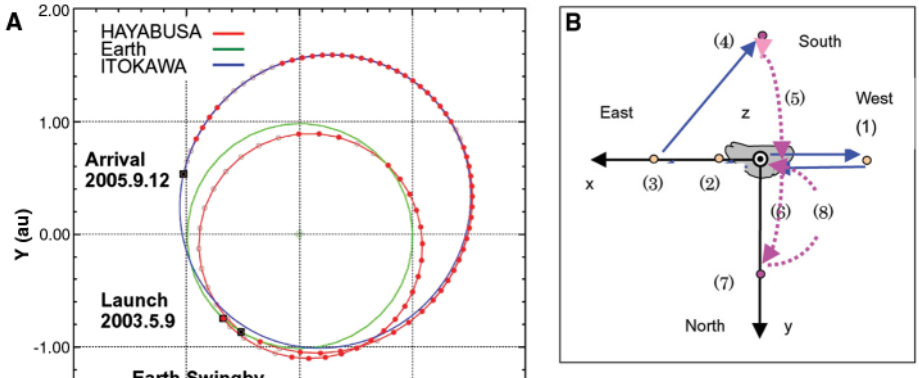


**Fig. 1.** (**A**) Trajectory of Hayabusa spacecraft to Itokawa. The view is looking down on the ecliptic plane from the north. The Sun is at (0,0). Red-dotted part along the spacecraft trajectory denotes the thrust direction of ion engines is northward, while other southward. (**B**) The spacecraft undertook a tour near the asteroid after achieving the home position observation. The view is from the Sun. The asteroid and the home position are overlapped at the origin. Arrows indicate the sequential path of the spacecraft. Dots show the hovering sites. Each spacecraft position indicated by the number in the figure corresponds to the dates that follow: position (1), 8 to 10 October, westward, high phase angle; (2), 12 and 13 October, zero solar phase angle; (3), 15 October, east side high, phase-angle; (4), 17 and 18 October, south pole; (5), 20 October, south pole, low altitude (~4 km); (6), 22 October, north pole, low altitude (~4 km); (7), 23 and 24 October, north pole; (8), 27 and 28 October, low altitude observation (~3 km). Dashed lines include low-altitude observation.

[1]Institute of Space and Astronautical Science (ISAS), Japan Aerospace Exploration Agency (JAXA), 3-1-1 Yoshinodai, Sagamihara, Kanagawa 229-8510, Japan. [2]Jet Propulsion Laboratory, California Institute of Technology, Pasadena, CA 91109, USA. [3]Graduate School of Science and Technology, Kobe University, 1-1 Rokkodai-cho, Nada, Kobe, Hyogo 657-8501, Japan. [4]Department of Aerospace Engineering, University of Michigan, Ann Arbor, MI 48109–2140, USA. [5]Applied Physics Laboratory, Johns Hopkins University, Laurel, MD 20723, USA. [6]School of Computer Science and Engineering, Aizu University, Ikki-machi, Aizu, Fukushima 965-8580, Japan. [7]NEC Aerospace Systems Limited, 4206 Ikebe, Tsuzuki, Yokohama, Kanagawa, 224-0053, Japan. [8]Department of Geosystem Engineering, University of Tokyo, Tokyo 113-8656, Japan. [9]Grid Technology Research Center (GTRC), National Institute of Advanced Industrial Science and Technology (AIST), Umezono 1-1-1, Tsukuba 305-8568, Japan. [10]Mizusawa Astrodynamics Observatory, National Astronomical Observatory of Japan, 2-12 Hoshigaoka, Mizusawa, Iwate 023-0861, Japan.

*To whom correspondence should be addressed. E-mail: fujiwara@planeta.sci.isas.jaxa.jp

continuous operation of the ion engines and an Earth swingby on 19 May 2004, the spacecraft arrived at an altitude of about 20 km (Gate position) near the sub-Earth point on 12 September 2005 (Fig. 1A). After a period of reconnaissance operation, the spacecraft transferred to the nominal hovering position (Home position) on 30 September 2005, at an altitude of about 7 km from the asteroid's surface and near the sub-Earth point.

Observational instruments onboard the Hayabusa spacecraft include a telescopic imaging camera (AMICA) with both a wide bandpass filter and seven narrowband filters, a near-infrared spectrometer (NIRS), a laser ranging instrument (LIDAR), and an x-ray fluorescence spectrometer (XRS). Specifications of these instruments are given in the following reports in this issue (*6*–*9*). A microrover named MINERVA (micro/nano experimental robot vehicle for asteroid), carrying a pair of stereoscopic imaging cameras, one short focal length camera, and thermal probes was released, but its landing onto the asteroid's surface was unsuccessful.

During 8 to 28 October 2005, the spacecraft left the home position and made tours to various altitudes and solar phase angles to access the polar regions and make high resolution topographic images under differing lighting conditions (Fig. 1B). On the basis of topographic and spectroscopic data, a surface sampling location on a smooth terrain called Muses Sea was selected. The touchdown, the 30-min stay on the asteroid surface, and the liftoff were performed on 19 and 25 November. At the time of the second touchdown, a small pellet should have been fired into the surface to get the ejected surface sample, but subsequent spacecraft telemetry suggests that the ignition for this shooting may not have occurred. In the first touchdown, however, there is a possibility that some surface material was flicked by the tip of the sampler and captured during the stay on the asteroid's surface. The return of the spacecraft and the sample capsule to Earth is now expected in June 2010, postponed from the original time of June 2007 because of problems with the chemical propulsion system.

Itokawa's fundamental parameters are summarized in Table 1. The pre-arrival results from ground-based observations (*2*–*5*) were all confirmed by the Hayabusa data within the observational uncertainties. The pole position was solved by tracking the ground control points on an AMICA image. There was no apparent short-term precession of the spin pole.

The mass of Itokawa was estimated from the Hayabusa tracking and navigation data by using different methods and data intervals. Initially, the mass was estimated by using range and Doppler data when Hayabusa moved from the gate position to home position (from 12 September to the beginning of October 2005). The estimated value was $3.51 \times 10^{10}$ kg with an uncertainty of 15%. The mass determination undertaken at this time suffered somewhat from errors because the effect of the radiation pressure was much larger than Itokawa's gravity. Therefore, we expected that we would be able to estimate the mass of Itokawa more accurately when Hayabusa approached Itokawa much more closely. However the second reaction wheel had a problem at the beginning of October 2005. After that, the chemical thrusters were used frequently to control the altitude, and this compromised subsequent mass determination attempts. On 21 and 22 October 2005, at a distance about 3 km from Itokawa, we intentionally stopped the altitude maneuvers and tried to estimate the mass of Itokawa by using Doppler, range, LIDAR, and optical data. The estimated mass was $3.43 \times 10^{10}$ kg with an uncertainty of 5%. The mass of Itokawa was also obtained on 12 November 2005, when the spacecraft approached Itokawa within a distance of 100 m. By using LIDAR data (*6*) as well as the navigation data and by considering the effects of attitude maneuvers, we estimated the mass of Itokawa during two orbit spans of this approach; the distances from Itokawa were 1400 to 800 m and 800 to 100 m. The estimated masses for these two spans were $3.58 \times 10^{10}$ kg with an uncertainty of 5% and $3.54 \times 10^{10}$ kg with an uncertainty of 6%, respectively. Therefore we have four separate estimations of Itokawa's mass, which are consistent within each estimation error. Calculating the weighted mean, we take the value of $3.51 \times 10^{10}$ kg as the most probable mass estimate. The uncertainty of this value is 3%.

The volume of Itokawa was estimated on the basis of the three-dimensional shape models created by the following three independent methods: (i) The limb profiling method, which integrates the outlines of images. This result is obtained most quickly and easily, but it cannot reproduce the concave surface areas. (ii) Stereogrammetry (multi-viewpoints' epipolar method). This model is constructed by using the stereometric views of representative points selected from the surface. The result depends on how the representative points can be appropriately extracted. (iii) Shaping from shading (photoclinometry). This model is constructed from the information on the surface brightness slopes, assuming the scattering properties of the surface are known. The volume adopted here is $1.84 \pm 0.092 \times 10^7$ m$^3$ (5% uncertainty) (*10*). Thus, the bulk density of Itokawa is $1.9 \pm 0.13$ g cm$^{-3}$.

Itokawa's shape resembles a sea otter (Fig. 2). It is composed of two parts; one is named the otter's "head" (smaller one) and the other is the otter's "body" (larger one) from their appearance (referred to hereafter as head and body). Both parts are not angular, like asteroid 951 Gaspra, but rather rounded. The appearance of the surface from the home position is, at first look, somewhat similar to the image of 433 Eros' surface at the same scale, but even in these images Itokawa's surface is still rougher and more boulder-rich. The Eros surface is globally covered with a thick regolith layer (*11*).

The surface of Itokawa is divided into rough terrain, mostly consisting of numerous boulders and smooth terrain (Muses Sea extending around the "neck" area between the head and body and

**Table 1.** Parameters for 25143 Itokawa. Osculating orbital elements are calculated from position and velocity at the specified time (Epoch – 2006 March 6.0 TDB, where TDB is barycentric dynamical time, TDB – UT = 65.2 seconds). These are from ground-based observations where $a$, $e$, $q$, $Q$, $\Omega$, $\omega$, $i$, and $T$ are the semi-major axis, eccentricity, perihelion distance, aphelion distance, longitude of the ascending node, argument of perihelion, and the perihelion passage time, respectively. $\beta$, $\lambda$ and RA, DEC are right ascension and declination in space and on the body, respectively.

| Property | Value |
|---|---|
| Osculating orbital elements | $a$ = 1.3238 AU $e$ = 0.2801<br>$\Omega$ = 69.0949° $\omega$ = 162.7526° $i$ = 1.6223°<br>$q$ = 0.9530 AU $Q$ = 1.6947 AU<br>$T$ = 2005 November 27.2169 TDB |
| Spectral type | S(IV) (*5*) |
| Size (diameter) | |
| Major axes | $x$ = 535 m, $y$ = 294 m, $z$ = 209 m (±1 m) |
| Osculating box size | 550 m by 298 m by 224 m (±1 m) |
| Rotational properties | |
| Period | 12.1324 ± 0.0001 hours (*31*) |
| Pole position | |
| in the space | [$\beta$,$\lambda$] = [–75° ± 12°, 320° ± 30°] (*3*)<br>[–84° ± 5°, 355°] (*2*)<br>[$\beta$,$\lambda$] = [128.5, –89.66] (J2000 ecliptic)<br>retrograde (±6.9°) |
| on the body | [RA, DEC] = [90.53, –66.30] (±6.9°)<br>(J2000 equator) |
| Volume | $1.84 \times 10^7 \pm 0.092 \times 10^7$ m$^3$ |
| Mass | $3.51 \times 10^{10} \pm 0.105 \times 10^{10}$ kg |
| Density | 1.9 ± 0.13 g cm$^{-3}$ |

Sagamihara around the north polar region). The smooth region is apparently similar to the Eros pond in the low resolution image, but it was found to be composed of fragmental debris with grain sizes of cm to mm scales from close-up images (*12*).

The largest boulder, Yoshinodai, is located near the end of the body and several boulders with sizes larger than a few tens of meters were found on the western side (180° to 360°E), whereas large boulders are less abundant on the eastern side. A black boulder exists at the end of the head and this feature marks the body's prime meridian. Large pinnacles are seen in the neck region on the western side associated with landslide-like topography (*7*). There is no substantial difference in mineralogical composition over the whole asteroid's surface in spite of the bifurcated appearance of Itokawa's shape (*8*, *9*).

The surface slopes, potential, and accelerations were computed by combining a polyhedral model of the Itokawa shape and the total estimated mass of the body. Assuming a constant density, the gravity field potential and acceleration at the surface can be evaluated analytically (*13*) and combined with the centripetal potential and acceleration to compute the amended potential, total acceleration, surface slope, and other dynamical quantities of interest (*14*). Figure 3 presents two such computations, the relative potential over the surface of the body and the surface slope over the body. It is noted that toward both end regions the potential becomes higher whereas low potential regions exist near the neck and northern areas on the body. There are two regional areas where the surface consistently has slopes less than 8°: an isolated region about the north pole and the Muses Sea area. In these regions, smooth terrain was observed and maintains its smoothness down to at least cm to mm sizes. A surface region with near-zero slopes can be considered locally to be an energetically relaxed shape, because the surface normal and the net acceleration acting at the region are approximately aligned with each other. This would be consistent with a loose granular layer in these regions that has been allowed to seek out its minimum energy. Hence, the accumulation of small grains could be explained by secondary movement of these grains on the surface through seismic shaking induced by impacts (*15*), shifting tidal loads from close planetary flybys, or perhaps electrostatic levitation for the finest sub-mm components if they exist (*16*). The existence of a thermally insulating layer consisting of gravels (*12*) in the smooth terrain and boulders in the rough terrain on the surface of Itokawa is also suggested by recent ground-based thermal inertia measurements (*17*). Itokawa's thermal inertia of 750 J $m^{-2}$ $s^{-0.5}$ $K^{-1}$ is more than an order of magnitude higher than that for large main-belt asteroids (5 to 25 J $m^{-2}$ $s^{-0.5}$ $K^{-1}$) and for the Moon (50 J $m^{-2}$ $s^{-0.5}$ $K^{-1}$).

Past impacts by interplanetary projectiles would have repeatedly fragmented and ejected Itokawa's surface material. Most of the finest ejecta particles would have velocities much higher than 10 to 20 cm $s^{-1}$ and would have easily escaped from Itokawa's surface. In impact experiments, the fragments having velocities less than this escape velocity are limited to a very small number of the largest fragments, with ejection being less effective for granular targets (*18*, *19*). Hence, one could suppose that finer particles are gradually lost as a result of impacts and the surface becomes covered with an abundance of larger boulders.

However, cm- to mm-sized regolith does exist on Itokawa's surface. One probable scenario is that such grains existed from the initial formation of the head and body and have been gradually depleted through cratering. Perhaps grains may be continuously produced if Itokawa is composed of boulder aggregates of various sizes with considerable macroporosity, at least near the surface. This structure would not only reduce the shock effect during impacts but also produce fine fragments in the shallow interior, if the characteristic size of the aggregate boulders is roughly comparable with the projectile sizes. Thus, a considerable amount of grains will be retained within the interior of the asteroid, and the fine particles can easily migrate through the larger boulders toward the low-potential regions like Muses Sea.

There is an empirical relationship between the size of a crater and the maximum size of the ejected fragment (*20*), which can well explain the relation of the largest boulder and the largest crater found on Eros (*21*). Following this empirical relationship, the size of the crater that would have produced the largest boulder, Yoshinodai, and some others actually exceeds the size of the largest craters found on Itokawa. Hence, these boulders are the likely relics formed in some cataclysmic event related to the formation of Itokawa's rough current shape.

Itokawa's bulk density of 1.9 g $cm^{-3}$ is considerably lower than the ~2.6 g $cm^{-3}$ determined for other S-type asteroids with well-determined bulk densities (*21*). Assuming that LL ordinary chondrites are reasonable analogs for Itokawa's composition (*8*) and a typical value for their bulk density is 3.2 g $cm^{-3}$ (*22*), the macroporosity of Itokawa is estimated to be ~41%. This value is substantially higher than the average value of ~30% for S-type asteroids, including Eros. Although it is not clear what the relative micro- and macroporosity values are, it is clear that Itokawa contains considerable void space in its interior. At least in terrestrial geology, porosities larger than 30% usually indicate loose soils or rubble (*22*).

The head and body are round in shape, rather than irregular as is typical for a monolithic fragment. This is also suggestive of the configuration that a rubble pile would preferentially evolve toward over long time intervals.

There are no conspicuous long linear structures extending nearly the entire length of the asteroid like the long ridge found on Eros (*23*), and this, coupled with the existence of some faint local facets with scales of at most several tens of meters, suggests that Itokawa is not a single consolidated, coherent body but rather an aggregate of rubble with sizes ranging up to about 50 m. It seems very likely that Itokawa has a rubble pile structure.

Careful observation of the head and body shows these surfaces are composed of many facets (*7*). In particular, the shape of the head looks like a polyhedron composed of many facets. Because the floors of craters formed on convex surfaces become flatter or even convex as the surface convexity increases (*24*), some of the facets observed on Itokawa could be of impact origin. The typical

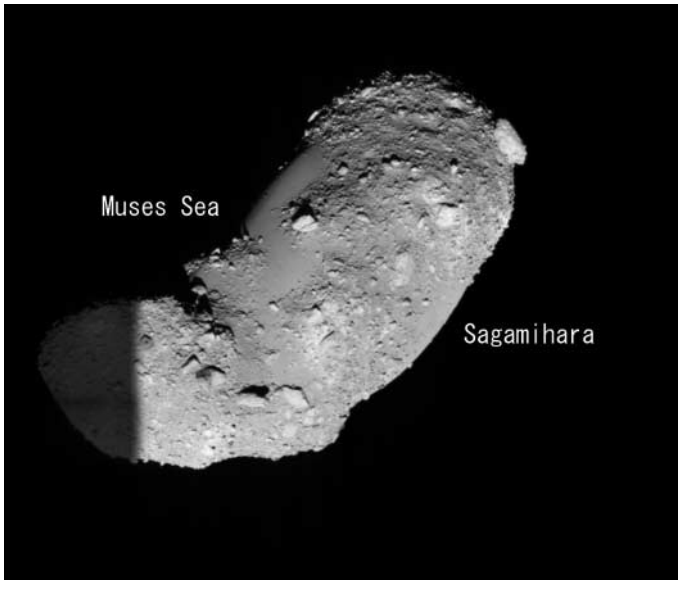


**Fig. 2.** Image of Itokawa taken at 7-km altitude taken from 6 km on 18 October (western side as seen from neighbor of south pole). Width of sight is 600 m.

example of this type is Little Woomera, a circular structure of diameter about 150 m extending around the end of the body (180°E). There is, however, a possibility that some facets could be the exposed surfaces of large fragments embedded near the asteroid's surface [for example, see the lateral side of the body in figure 2 in (*10*)].

If Itokawa was once a coherent body, it might have experienced collisional disruption followed by re-agglomeration. Hence, Itokawa could be either a young object or a loosely consolidated body, or both. Few asteroids as large as, or larger than, Itokawa are fast rotators, and this evidence has been used to argue that most asteroids larger than about 150 m may be rubble piles (*25*).

The existence of large facets and many boulders implies that Itokawa has experienced a number of large impacts (paucity of craters is due to shaking, and this does not deny many past impacts). If the asteroid is a gravitationally aggregated body and has large macroporosity, impact shocks should not be transmitted effectively (*26*), which would suppress further impact disruptions.

Landslide-like deposits at the base of the head are observed (*10*), and this region has slopes in excess of 35° (Fig. 2B). On Itokawa, most angular grain materials have an angle of repose on the order of 32° to 35°, and slope angles in excess of this height cannot be maintained unless there is cohesion. The observation of the candidate landslide, and the fact that the steep slopes on the head measure up to near 50°, may suggest that at least this region resulted from an angular rubble pile that collapsed.

Itokawa looks to be composed of two parts, the head and the body. There are plausible origin scenarios to produce such a bifurcated configuration.

The first scenario is the contacted bodies hypothesis: Originally the head and body could have formed separately and later come into contact at a slow relative speed, and, almost retaining the original shape of both bodies but with some mass movement, the present shape of Itokawa was formed. Between the head and body, a depressed neck zone is observed, and in this region there is a high-slope region (expressed as yellow in Fig. 3B) that suggests that the head was once an independent body and that the material has not yet completely relaxed into the neck region. The prominent ridge in Muses Sea near the south side of the neck may have originated from the collision of the head and the body. The different orientations of the principal axes of the head and body (*7*) also imply these bodies were originally separate and were produced by a slow collision between the head and body. The likely scenarios for the origin of the contacted body would include the following: (i) Formation by capture of two independent asteroids. This is in fact unlikely because of the low probability of encounters at relative velocities lower than the crushing velocity, and there is no hard evidence that strongly suggests that the head and body originated from two independent asteroids. (ii) Mutual capture of two fragments after catastrophic disruption of a larger parent body, which might be possible, as indicated by numerical modeling results (*26*). However, capture scenarios may have difficulty accounting for the ellipsoidal shapes of the head and the body. (iii) Mutual agglomeration after a catastrophic breakup of the parent body. The flying fragments agglomerated (*27*), forming some rubble-pile bodies, two of which may have co-orbited around one another and, after development of the ellipsoidal shapes, then came into contact as a result of some unknown event, for example, after a close planetary encounter (*28*). (iv) Rotational fission due to an excessive spin rate, which however is not consistent with the currently observed spin rate. (v) Mass shedding resulting from tidal disruption during a close planetary encounter.

Another possible scenario for the formation of the depressed neck region includes it being formed by a large impact. In this scenario, the body originally existed as a single entity and a large impact formed the depression presently seen at the neck region on Itokawa. Impact experiments suggest that a large impact on the lateral side of an elongated body could produce a saddle-like depression (*24*). It is plausible that an impact could cause a large breakage at the neck region or perhaps separate the body into two parts (body and head). Then both bodies could have settled back together, forming the present shape of Itokawa.

The properties of Itokawa found by Hayabusa, such as its being boulder-rich and with a rubble pile structure, may be common for small S-type asteroids because Itokawa does not belong to any special category with respect to parameters such as spectra, rotational period, and orbital

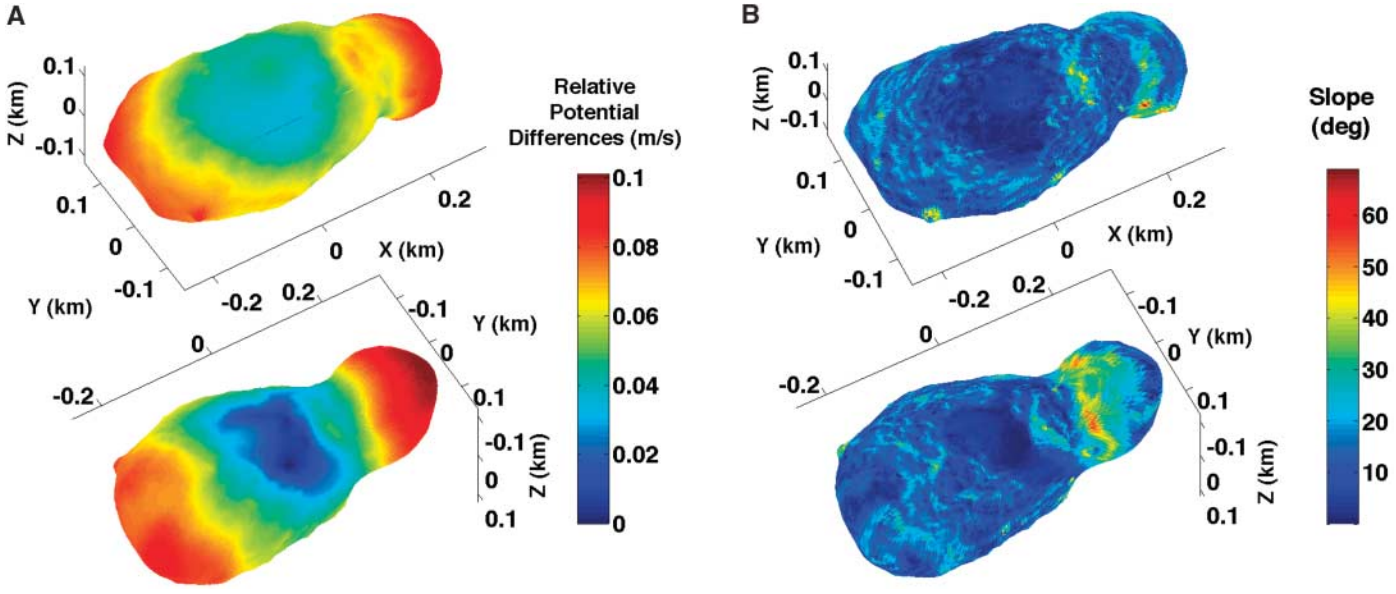


**Fig. 3.** (**A**) Relative gravitational and rotational potential mapped onto an Itokawa shape model. This plot measures the speed needed to energetically transition from the lowest potential point on Itokawa to any other region (*30*). Conversely, it measures the speed a particle dropped with zero speed at that location if it fell unimpeded to the lowest potential point on Itokawa, which is situated within the Muses Sea region. Top and bottom views show the northern and southern hemisphere, respectively. (**B**) Surface slopes mapped onto an Itokawa shape model. The slopes are defined as the supplement of the angle between the local surface normal and the total gravitational and rotational acceleration acting on a particle at that surface location (*14*). Upper and lower views show northern and southern hemispheres, respectively.

elements. Moreover, it should also be noted that elongated asteroids and binary asteroids are numerous among the near-Earth asteroid population (*29*) and that these characteristics are consistent with these objects evolving into contact binary systems. In this sense, the Hayabusa results provide a benchmark for understanding general properties of small asteroids.

### References and Notes


1. J. Kawaguchi *et al.*, *Acta Astronaut.* **52**, 117 (2003).
2. M. Kaasalainen *et al.*, *Astron. Astrophys.* **405**, L29 (2003).
3. Y. Ohba *et al.*, *Earth Planets Space* **55**, 341 (2003).
4. S. J. Ostro *et al.*, *Meteorit. Planet. Sci.* **39**, 407 (2004).
5. R. J. Binzel *et al.*, *Meteorit. Planet. Sci.* **36**, 1167 (2001).
6. S. Abe *et al.*, *Science* **312**, 1344 (2006).
7. J. Saito *et al.*, *Science* **312**, 1341 (2006).
8. M. Abe *et al.*, *Science* **312**, 1334 (2006).
9. T. Okada *et al.*, *Science* **312**, 1338 (2006).
10. H. Demura *et al.*, *Science* **312**, 1347 (2006).
11. C. R. Chapman *et al.*, *Icarus* **155**, 104 (2002).
12. H. Yano *et al.*, *Science* **312**, 1350 (2006).
13. R. A. Werner, D. J. Scheeres, *Celestial Mech. Dyn. Astron.* **65**, 313 (1997).
14. D. J. Scheeres, S. J. Ostro, R. S. Hudson, R. A. Werner, *Icarus* **121**, 67 (1996).
15. A. F. Cheng *et al.*, *Meteor. Planet. Sci.* **37**, 1095 (2002).
16. P. Lee *et al.*, *Icarus* **124**, 181 (1996).
17. T. G. Mueller *et al.*, *Astron. Astrophys.* **443**, 347 (2005).
18. A. Nakamura *et al.*, *Icarus* **92**, 132 (1991).
19. E. Asphaug *et al.*, in *Asteroids III*, W. F. Bottke Jr., A. Cellino, P. Paolicchi, R. P. Binzel, Eds. (Univ. Arizona Press, Tucson, AZ, 2002), pp. 463–484.
20. D. E. Gault *et al.*, *NASA Technical Document* **TND-1767**, 39 (1963).
21. P. C. Thomas *et al.*, *Nature* **413**, 394 (2001).
22. D. T. Britt *et al.*, in *Asteroids III*, W. F. Bottke Jr., A. Cellino, P. Paolicchi, R. P. Binzel, Eds. (Univ. Arizona Press, Tucson, AZ, 2002), pp. 485–500.
23. J. Veverka *et al.*, *Science* **278**, 2109 (1997).
24. A. Fujiwara *et al.*, *Icarus* **105**, 345 (1993).
25. R. J. Whitely *et al.*, *Icarus* **157**, 157 (2002).
26. E. Asphaug *et al.*, *Nature* **393**, 437 (1998).
27. P. Michel *et al.*, *Nature* **421**, 608 (2003).
28. P. Michel *et al.*, *Icarus* **179**, 291 (2005).
29. W. J. Merline *et al.*, in *Asteroids III*, W. F. Bottke Jr., A. Cellino, P. Paolicchi, R. P. Binzel, Eds. (Univ. Arizona Press, Tucson, AZ, 2002), pp. 289–312.
30. The gravitational plus rotational potential is defined by the Jacobi integral of the system: $J = V^2/2 - U(r)$, where $U$ is the gravitational plus centripetal force potential, $r$ defines a location on the surface of the body, and $V$ is the speed of a particle relative to the rotating body frame (*14*). The gravitational plus rotational potential is defined as the value of $J$ evaluated for zero speed or the value of $-U(r)$ over the surface of the body. The speed necessary to have sufficient energy to travel from the lowest point of the potential [largest value of $U(r)$ at location $r^*$] to any other point $r$ on the surface of the body is then $\sqrt{2[U(r^*) - U(r)]}$, which is plotted in the figure.
31. S. Nishihara *et al.*, *Lunar Planet. Sci. Conf.* **XXXVI**, abstr. 1833 (2005).


32. We thank the mission operation and spacecraft team of the Hayabusa project at ISAS/JAXA for their efforts that resulted in making Hayabusa the first Japanese spacecraft rendezvoused and landed at the asteroid. This research was supported by ISAS/JAXA, NASA, Kobe University through the 21st Century COE Program of the Origin and Evolution of Planetary Systems, and University of Aizu. A portion of the research reported in this paper was performed at the Jet Propulsion Laboratory, California Institute of Technology, under a contract with NASA.

6 February 2006; accepted 6 April 2006
10.1126/science.1125841


REPORT

# Near-Infrared Spectral Results of Asteroid Itokawa from the Hayabusa Spacecraft


**M. Abe,[1] Y. Takagi,[2] K. Kitazato,[1,3] S. Abe,[4] T. Hiroi,[5] F. Vilas,[6] B. E. Clark,[7] P. A. Abell,[8] S. M. Lederer,[9] K. S. Jarvis,[8,10] T. Nimura,[1,3] Y. Ueda,[3] A. Fujiwara[1]**



**The near-infrared spectrometer on board the Japanese Hayabusa spacecraft found a variation of more than 10% in albedo and absorption band depth in the surface reflectance of asteroid 25143 Itokawa. Spectral shape over the 1-micrometer absorption band indicates that the surface of this body has an olivine-rich mineral assemblage potentially similar to that of LL5 or LL6 chondrites. Diversity in the physical condition of Itokawa's surface appears to be larger than for other S-type asteroids previously explored by spacecraft, such as 433 Eros.**


Visible and near-infrared spectroscopic observations (from 0.3 to 3.3 μm) have been used extensively to study the mineralogy and physical properties of asteroid surfaces. These data are compared with similar laboratory measurements of meteorites from asteroids to determine the geologic history of the asteroid regions. Because most of the asteroids have not experienced major mineralogical alteration since the formation of the solar system, study of their chemical and physical properties tells us about the earliest epochs of planet formation. Asteroid 25143 Itokawa (previously 1998 SF36) has been observed unresolved from ground-based telescopes at mineralogically diagnostic wavelengths (*1*, *2*) and has been found to be similar to ordinary chondrite and/or primitive achondrite meteorites. Here, we report spectral observations of Itokawa at high spatial resolution and place them in the context of their geologic interpretation.

The near-infrared spectrometer (NIRS) onboard the Japanese Hayabusa spacecraft (also known as MUSES-C) obtained more than 80,000 spectra of asteroid Itokawa during mapping operations at the asteroid from September to November 2005. NIRS has a 64-channel InGaAs photodiode array detector and a grism (a diffraction grating combined with a prism). The dispersion per pixel is 23.6 nm. Spectra were collected from 0.76 to 2.1 μm (*3*). The NIRS field of view (0.1° × 0.1°) was aligned with the LIDAR (Light Detection and Ranging) and the AMICA (Asteroid Multiband Imaging Camera) fields of view before launch. During the cruising and mapping phases, this coalignment was verified multiple times.

The first spectrum from Itokawa was obtained by NIRS on 10 September 2005 at a distance of 50 km from the asteroid. NIRS spectra were obtained at solar phase angles ranging from near 0° to 38° and at footprint sizes ranging from 6 to 90 $m^2$ (not including the touchdown phase of the mission). Most spectra were obtained between 7° and 11° solar phase angle during the first mapping phase of the mission in September.

During this mapping phase, while the spacecraft was 7 to 20 km from the asteroid, an equatorial scan was performed using only the rotation of the asteroid to shift the pointing of NIRS. During the second mapping phase in October 2005, a two-dimensional scan was obtained by slewing the attitude of the spacecraft in the direction of the rotational axis of the asteroid. The spacecraft hovered at a distance of 3.5 to 7 km above the asteroid during this time. The position of the spacecraft was limited to near 0° Earth phase angle during the first mapping phase, but after arriving at a distance of 7 km from the asteroid's surface, the spacecraft was moved off the Earth-asteroid line to vary the solar phase angle and aspect angle while observations were performed.

Itokawa's phase curve (brightness as a function of varying solar phase angle) at NIRS wavelengths can be compared to phase curves of


[1]Institute of Space and Astronautical Science, Japan Aerospace Exploration Agency, 3-1-1 Yoshinodai, Sagamihara, Kanagawa 229-8510, Japan. [2]Toho Gakuen University, 3-11 Heiwagaoka, Meito, Nagoya, Aichi 465-8515, Japan. [3]University of Tokyo, 7-3-1 Hongo, Bunkyo, Tokyo 113-0033, Japan. [4]Graduate School of Science and Technology, Kobe University, 1-1 Rokkodai, Nada, Kobe, Hyogo 657-8501, Japan. [5]Department of Geological Science, Brown University, Providence, RI 02912, USA. [6]MMT Observatory, Post Office Box 210065, University of Arizona, Tucson, AZ 85721, USA. [7]Department of Physics, Ithaca College, Ithaca, NY 14850, USA. [8]National Aeronautics and Space Administration, Lyndon B. Johnson Space Center, Houston, TX 77058, USA. [9]Department of Physics, California State University, 5500 University Parkway, San Bernardino, CA 92407, USA. [10]ESC Group/Hamilton Sundstrand, 2224 Bay Area Boulevard, Houston, TX 77058, USA.